Article:

Yang, F. orcid.org/0000-0002-6428-7755, Dean, J.S. orcid.org/0000-0001-7234-1822, Hu, Q. orcid.org/0000-0001-7639-9239 et al. (4 more authors) (2020) From insulator to oxide-ion conductor by a synergistic effect from defect chemistry and microstructure: acceptor-doped Bi-excess sodium bismuth titanate Na0.5Bi0.51TiO3.015. Journal of Materials Chemistry A, 8 (47). pp. 25120-25130. ISSN 2050-7488

https://doi.org/10.1039/d0ta10071d

Supplementary information

From insulator to oxide-ion conductor by a synergistic effect from defect chemistry and microstructure: acceptor-doped Bi-excess sodium bismuth titanate $Na_{0.5}Bi_{0.51}TiO_{3.015}$

Fan Yang[1,*], Julian S. Dean[2], Qiaodan Hu[3], Patrick Wu[2], Emilio Pradal-Velázquez[2], Linhao Li[2] and Derek C Sinclair[2,*]

[1] Institute of Fuel Cells, School of Mechanical Engineering, Shanghai Jiao Tong University, 800 Dongchuan Road, Minhang District, Shanghai, 200240, P. R. China.

[2] Department of Materials Science and Engineering, University of Sheffield, Sir Robert Hadfield Building, Mappin Street, Sheffield, S1 3JD, UK.

[3] School of Materials Science and Engineering, Shanghai Jiao Tong University, 800 Dongchuan Road, Minhang District, Shanghai, 200240, P. R. China

*Corresponding authors. fanyang_0123@sjtu.edu.cn; d.c.sinclair@sheffield.ac.uk.

1. XRD patterns of other acceptor-doped $NB_{0.51}T$ ceramics

XRD patterns of $Na_{0.5}Bi_{0.51}Ti_{1-y}N_yO_{3.015-0.5y}$ (N = Sc, Al and Ga) ceramics are shown in Figs. S1-S3. Sc-doped $NB_{0.51}T$ ceramics are phase pure within the composition range investigated ($y \leq 0.05$). For Al- and Ga-doped $NB_{0.51}T$, peaks from secondary phases can be observed for *y* = 0.05 and 0.07, respectively.

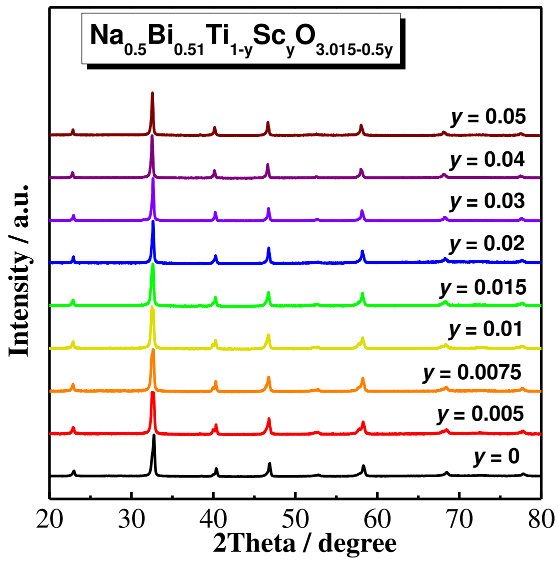

Fig.S1 XRD patterns of $Na_{0.5}Bi_{0.51}Ti_{1-y}Sc_yO_{3.015-0.5y}$ (y = 0, 0.005, 0.0075, 0.01, 0.015, 0.02, 0.03, 0.04 and 0.05) ceramics.

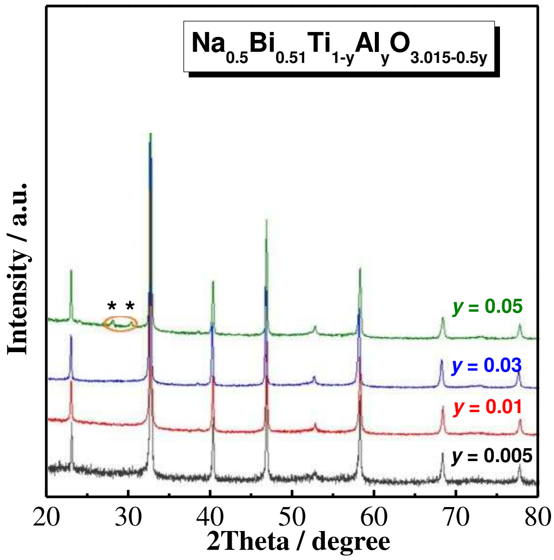

Fig.S2 XRD patterns of $Na_{0.5}Bi_{0.51}Ti_{1-y}Al_yO_{3.015-0.5y}$ (y = 0.005, 0.01, 0.03 and 0.05) ceramics. The star symbol indicates the presence of a secondary phase(s) for y = 0.05.

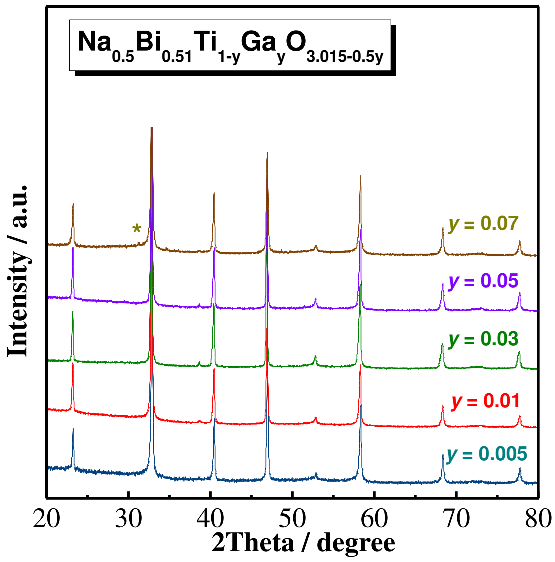

Fig.S3 XRD patterns of $Na_{0.5}Bi_{0.51}Ti_{1-y}Ga_yO_{3.015-0.5y}$ (y = 0.005, 0.01, 0.03, 0.05 and 0.07) ceramics. The star symbol indicates the presence of a secondary phase for y = 0.07.

2. Microstructure of $NB_{0.51}T$ and grain size distribution in Mg-doped $NB_{0.51}T$ ceramics

Undoped $NB_{0.51}T$ ceramics have uniform, small grains with an average grain size of ~ 1-2 μm (Fig. S4(a)). To make sure the thermal-etched surface morphology can represent the bulk, the grain structure is also observed from the cross-sectional, fracture surface (Fig.S4(b)). It also shows uniform, small grains and therefore confirms the surface grain structure is representative. In this work, statistics of grain size is based on the thermal-etched surface for easy comparison with those reported in literature. For Mg-doped $NB_{0.51}T$ ceramics the grain size shows an increasingly broad distribution with increasing doping level (x), as well as an increase in the average value (Fig. S5).

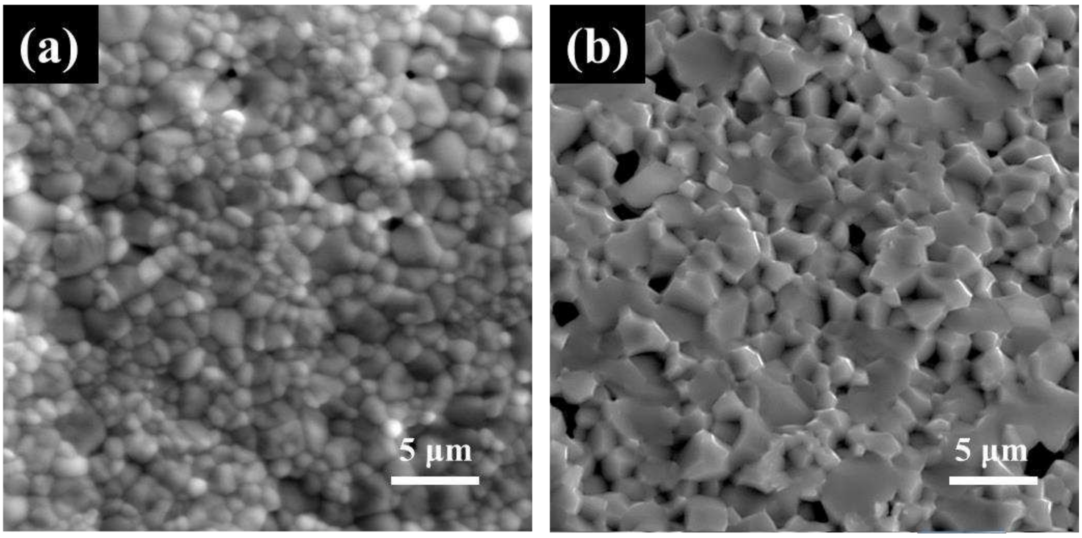

Fig.S4 SEM images of an $NB_{0.51}T$ ceramic: (a) thermal-etched surface and (b) fracture surface.

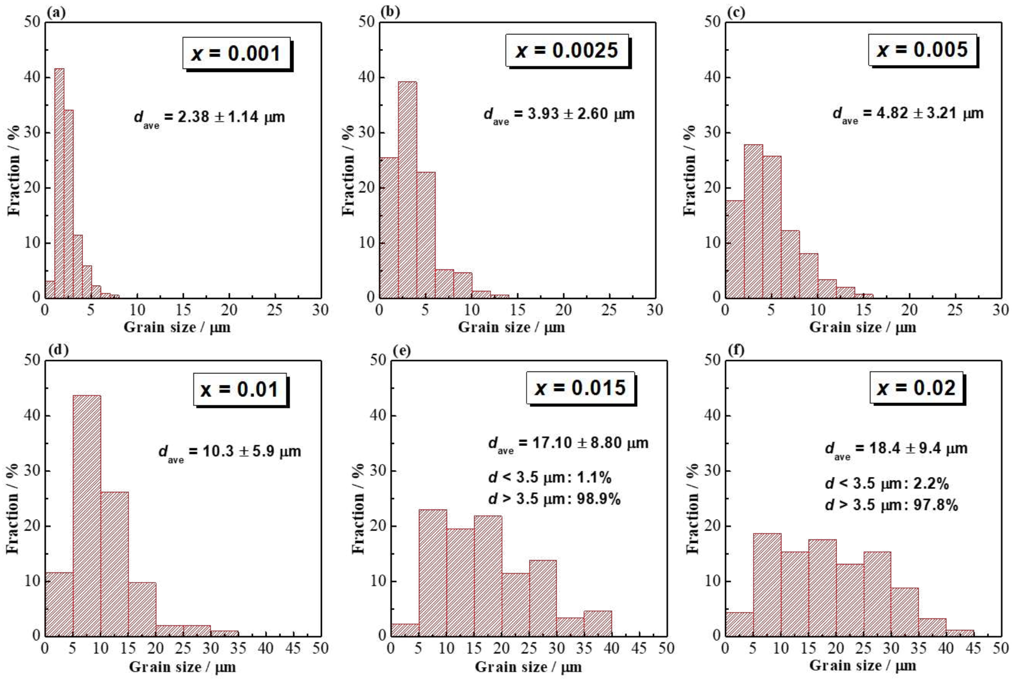

Fig. S5 Grain size distribution in $Na_{0.5}Bi_{0.51}Ti_{1-x}Mg_xO_{3.015-x}$ ceramics. (a) x = 0.001, (b) x = 0.0025, (c) x = 0.005, (d) x = 0.01, (e) x = 0.015 and (f) x = 0.02. Average grain size and its associated error is indicated in each figure.

3. Microstructure of other acceptor-doped $NB_{0.51}T$ ceramics

$NB_{0.51}T$ ceramics doped with other B-site acceptor-dopants show similar inhomogeneous distributions of large grains embedding in small grains at low doping levels, as shown in Fig.S6 for Zn and Fig.S7 for Sc. With increasing doping level *y*, the grain size of Sc-doped $NB_{0.51}T$ ceramics increases.

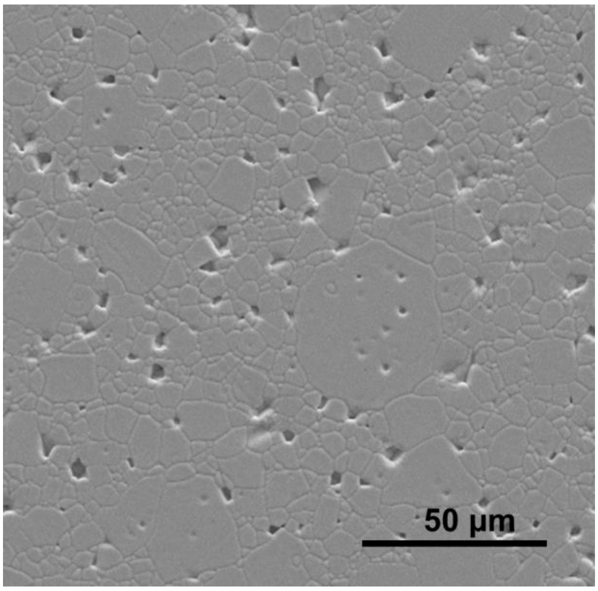

Fig. S6 SEM image of a thermally-etched surface of $Na_{0.5}Bi_{0.51}Ti_{1-x}Zn_xO_{3.015-x}$ (x = 0.005).

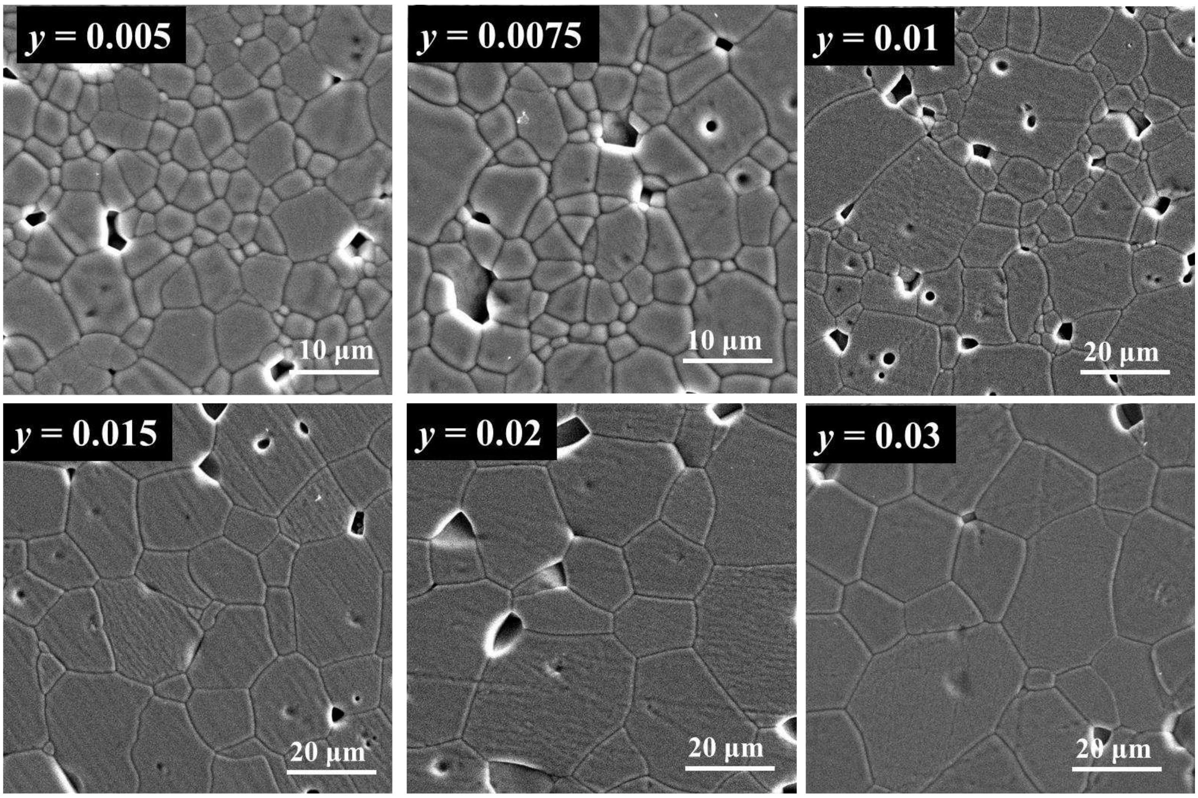

Fig.S7 SEM micrographs of thermally-etched surfaces of $Na_{0.5}Bi_{0.51}Ti_{1-y}Sc_yO_{3.015-0.05y}$ (y = 0.005, 0.0075, 0.01, 0.015, 0.02 and 0.03).

4. Compositional analysis of a thermally-etched Zn-doped $NB_{0.51}T$ (x = 0.005) ceramic

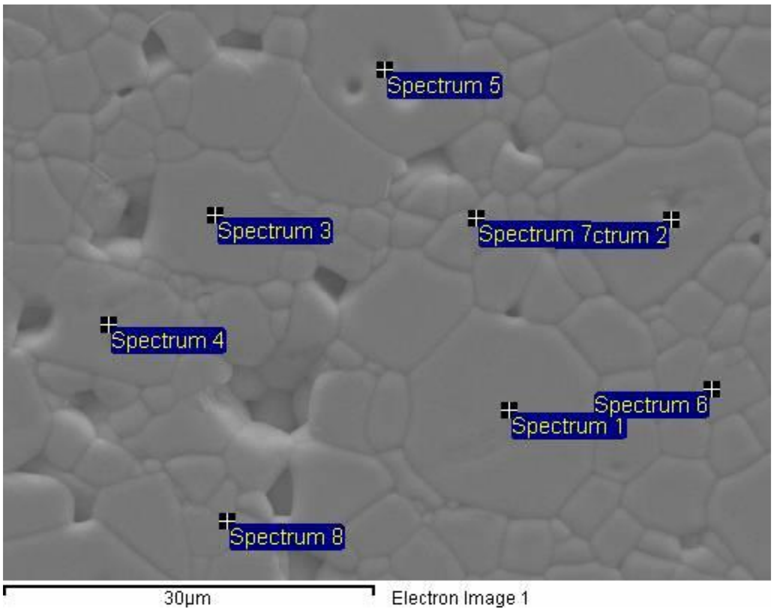

Table S1 Relative atomic percentage of cations in x = 0.005 $Na_{0.5}Bi_{0.51}Ti_{1-x}Zn_xO_{3.015-x}$ ceramics measured by EDS.

Position	Na	Bi	Ti	Zn
1	23.29	26.76	49.80	0.15
2	26.18	26.35	47.77	-0.30
3	25.12	26.46	47.97	0.45
4	23.45	26.91	49.08	0.55
5	24.74	26.26	48.90	0.10
6	25.37	26.17	47.86	0.60
7	22.04	27.21	50.75	0
8	24.12	26.80	49.34	-0.25
Average	24.29 ± 1.30	26.62 ± 0.36	48.93 ± 1.04	0.16 ± 0.35
Nominal	24.88	25.37	49.50	0.25

5. Bulk conductivity of Zn, Sc, Al and Ga-doped $NB_{0.51}T$ ceramics

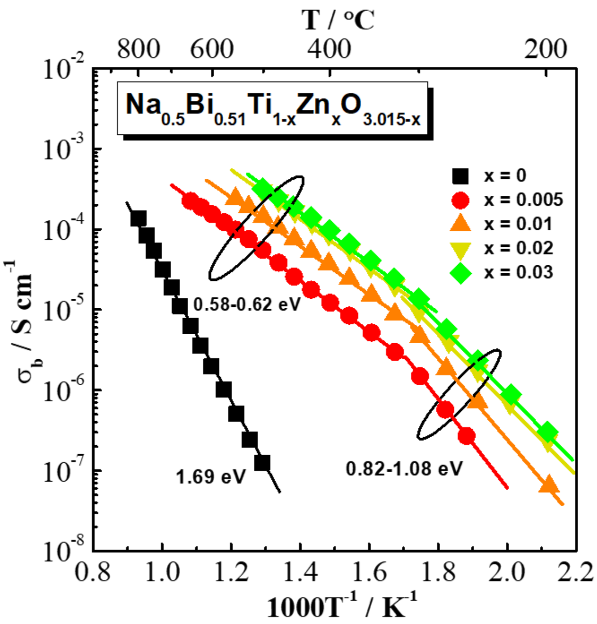

Fig.S8 Arrhenius plot of bulk conductivity, σ_b, for $Na_{0.5}Bi_{0.51}Ti_{1-x}Zn_xO_{3.015-x}$ (x = 0, 0.005, 0.01, 0.02 and 0.03) ceramics measured in air. Numbers in eV are the activation energies associated with σ_b.

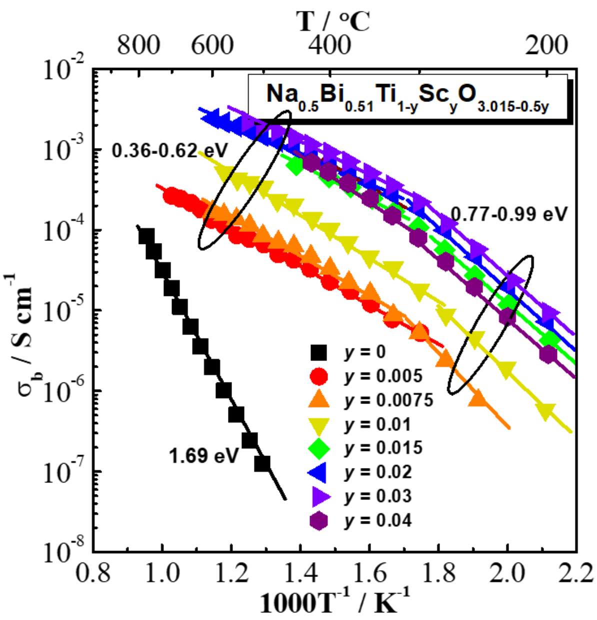

Fig.S9 Arrhenius plot of bulk conductivity, σ_b, for $Na_{0.5}Bi_{0.51}Ti_{1-y}Sc_yO_{3.015-0.5y}$ (y = 0, 0.005, 0.0075, 0.01, 0.015, 0.02, 0.03 and 0.04) ceramics measured in air. Numbers in eV are the activation energies associated with σ_b.

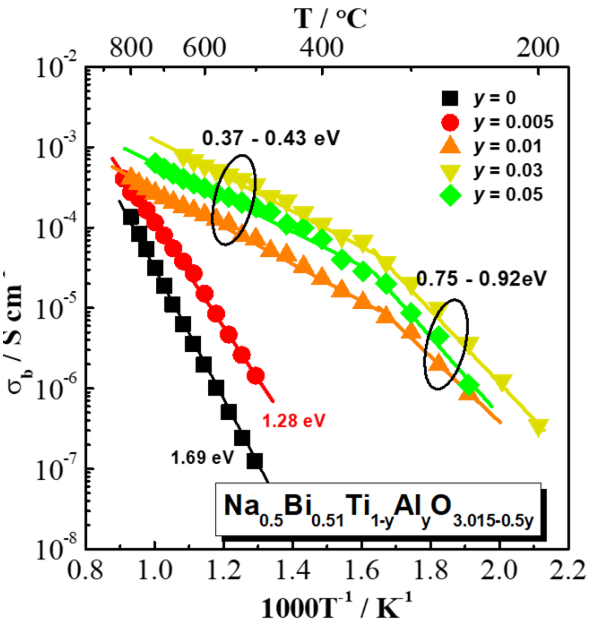

Fig.S10 Arrhenius plot of bulk conductivity, σ_b, for $Na_{0.5}Bi_{0.51}Ti_{1-y}Al_yO_{3.015-0.5y}$ (y = 0, 0.005, 0.01, 0.03 and 0.05) ceramics measured in air. Numbers in eV are the activation energies associated with σ_b.

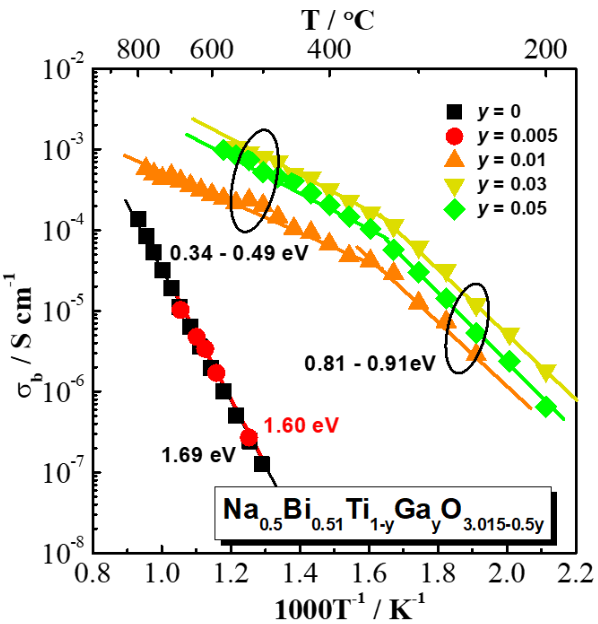

Fig.S11 Arrhenius plot of bulk conductivity, σ_b, for $Na_{0.5}Bi_{0.51}Ti_{1-y}Ga_yO_{3.015-0.5y}$ (y = 0, 0.005, 0.01, 0.03 and 0.05) ceramics measured in air. Numbers in eV are the activation energies associated with σ_b.

4. Dielectric properties of Zn, Sc, Al and Ga-doped $NB_{0.51}T$ ceramics

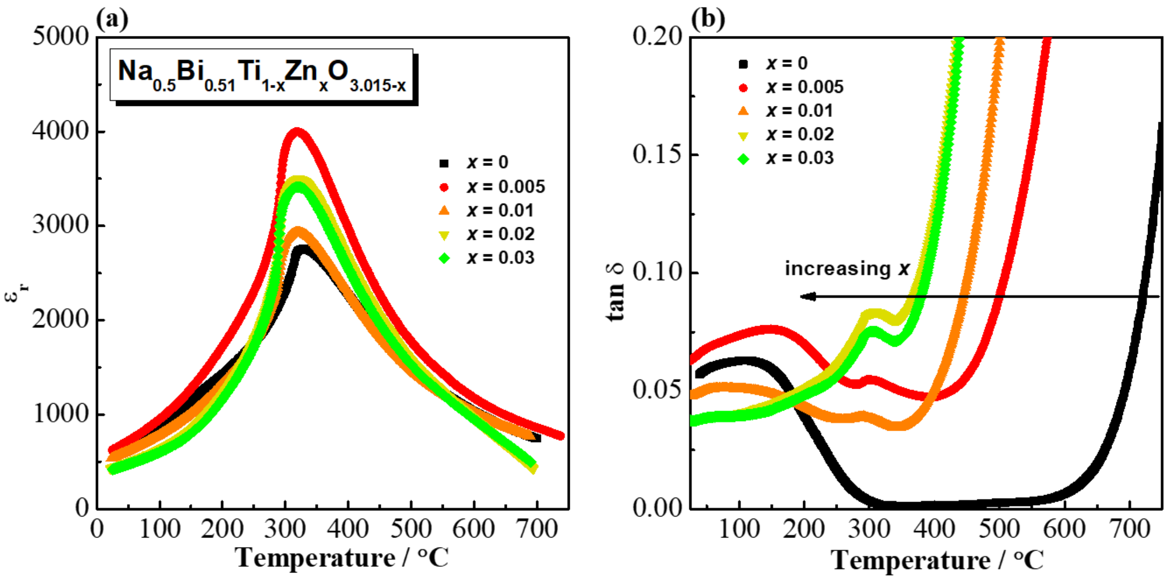

Fig.S12 Dielectric spectroscopy for $Na_{0.5}Bi_{0.51}Ti_{1-x}Zn_xO_{3.015-x}$ (x = 0, 0.005, 0.01, 0.02 and 0.03) ceramics: (a) permittivity at 1 MHz versus temperature and (b) dielectric loss, tan δ, (1 MHz) versus temperature.

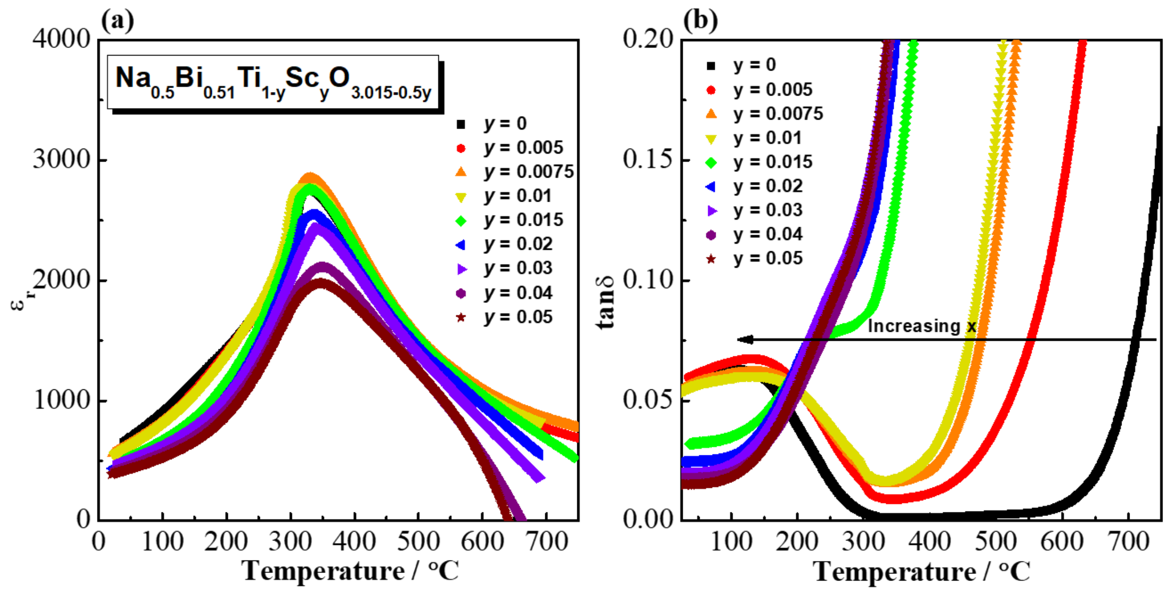

Fig.S13 Dielectric spectroscopy for $Na_{0.5}Bi_{0.51}Ti_{1-y}Sc_yO_{3.015-0.5y}$ (y = 0, 0.005, 0.0075, 0.01, 0.015, 0.02, 0.03, 0.04 and 0.05) ceramics: (a) permittivity at 1 MHz versus temperature and (b) dielectric loss, tan δ, (1 MHz) versus temperature.

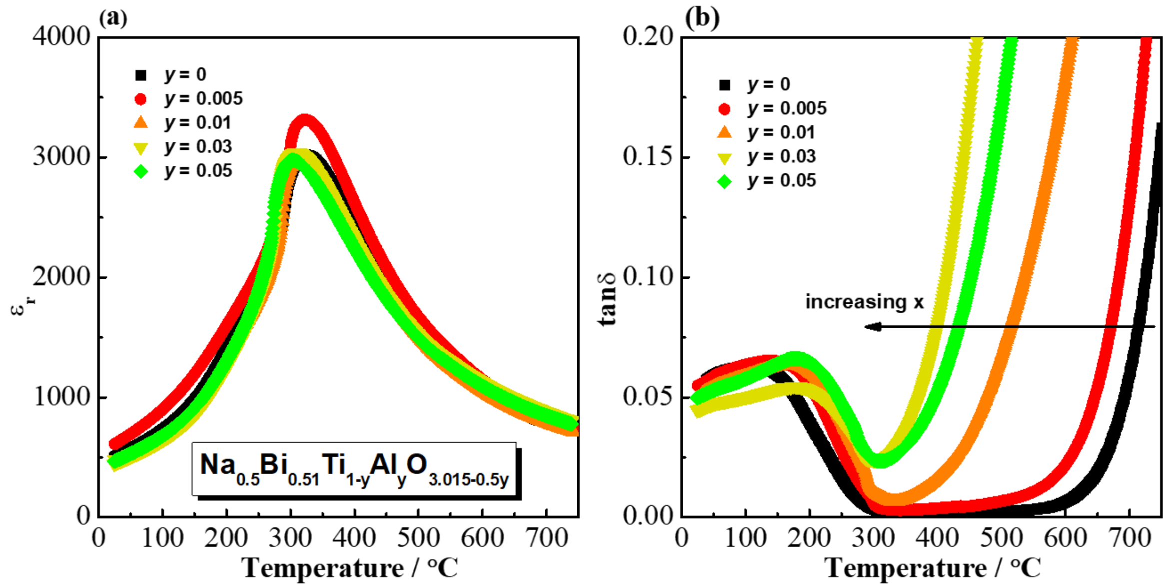

Fig.S14 Dielectric spectroscopy for $Na_{0.5}Bi_{0.51}Ti_{1-y}Al_yO_{3.015-0.5y}$ (y = 0, 0.005, 0.01, 0.03 and 0.05) ceramics: (a) permittivity at 1 MHz versus temperature and (b) dielectric loss, tan δ, (1 MHz) versus temperature.

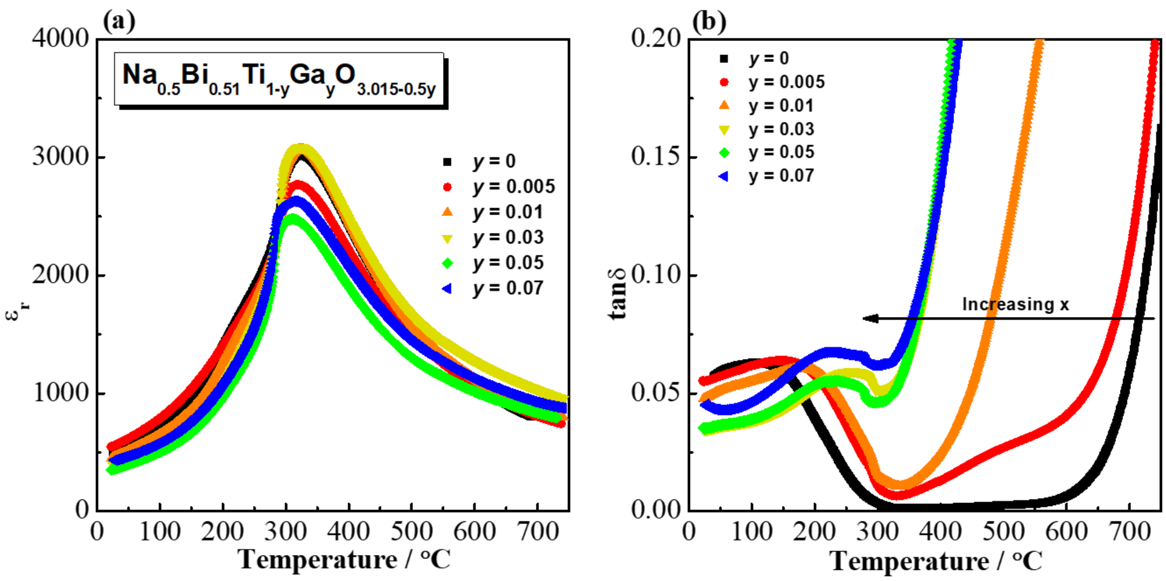

Fig.S15 Dielectric spectroscopy for $Na_{0.5}Bi_{0.51}Ti_{1-y}Ga_yO_{3.015-0.5y}$ (y = 0, 0.005, 0.01, 0.03, 0.05 and 0.07) ceramics: (a) permittivity at 1 MHz versus temperature and (b) dielectric loss, tan δ, (1 MHz) versus temperature.